

The Role of Plastocyanin in the Adjustment of the Photosynthetic Electron Transport to the Carbon Metabolism in Tobacco¹

Mark Aurel Schöttler*, Helmut Kirchhoff, and Engelbert Weis

Institut für Botanik, Westfälische Wilhelms-Universität, 48 149 Munster, Germany

We investigated adaptive responses of the photosynthetic electron transport to a decline in the carbon assimilation capacity. Leaves of different ages from wild-type tobacco (*Nicotiana tabacum*) L. var Samsun NN and young mature leaves of tobacco transformants with impaired photoassimilate export were used. The assimilation rate decreased from 280 in young mature wild-type leaves to below 50 mmol electrons mol chlorophyll⁻¹ s⁻¹ in older wild-type leaves or in transformants. The electron transport capacity, measured in thylakoids isolated from the different leaves, closely matched the leaf assimilation rate. The numbers of cytochrome (cyt)-*bf* complexes and plastocyanin (PC) decreased with the electron transport and assimilation capacity, while the numbers of photosystem I (PSI), photosystem II, and plastoquinone remained constant. The PC to PSI ratio decreased from five in leaves with high assimilation rates, to values below one in leaves with low assimilation rates, and the PC versus flux correlation was strictly proportional. Redox kinetics of cyt-*f*, PC, and P₇₀₀ suggest that in leaves with low electron fluxes, PC is out of the equilibrium with P₇₀₀ and cyt-*f* and the cyt-*f* reoxidation rate is restricted. It is concluded that the electron flux is sensitive to variations in the number of PC, relative to PSI and cyt-*bf*, and PC, in concert with cyt-*bf*, is a key component that adjusts to control the electron transport rate. PC dependent flux control may serve to adjust the electron transport rate under conditions where the carbon assimilation is diminished and thereby protects PSI against over-reduction and reactive oxygen production.

In the light, NADPH and ATP are produced by the photosynthetic electron transport chain (ETC). These products are consumed by metabolic reactions, mainly the Calvin cycle, where the photosynthetic flux is partitioned between carbon assimilation and photorespiration. In saturating light, the overall flux depends on the Calvin cycle activity, which itself is controlled by the Rubisco activity and the carbon flux into starch or Suc synthesis. If the carbon flux in the plant is diminished by a restriction of export and consumption of carbohydrates (sink limitation), the capacity of the thylakoid-bound light reactions could exceed the demand by the Calvin cycle. The photo-reactions at PSI and PSII are exergonic and virtually irreversible and potentially destructive processes. Excess electrons, deliberated at PSII from water and delivered to PSI and not used by the carbon reactions, could be transferred to alternative acceptors, among them O₂ (Backhausen et al., 2000; Foyer and Noctor, 2000; Ort and Baker, 2002). Reduction of molecular O₂ at PSI leads to the production of the superoxide radical (O₂⁻), a strong oxidant, and other reactive oxygen species (ROS). To some extent, ROS produced in the light can be detoxified through the Mehler-Asada

cycle, so that, over a certain range of physiological conditions, no oxidative damage to the photosynthetic apparatus occurs (Asada, 1999). However, at least in C₃ plants, the capacity of the Mehler-Asada cycle may not exceed about 10% of the capacity of the photosynthetic electron transport (PET; Badger et al., 2000). Similarly, other potential overflow valves for excess electrons, such as the oxaloacetate/malate shuttle (Backhausen et al., 2000), are limited in their capacity. Furthermore, these overflow reactions do not consume ATP and, hence, do not serve to dissipate the proton motive force that is built up by the light-driven proton pumping across the thylakoid membrane. Thus, if the capacity of light reactions and PET exceeds that of the electron consuming reactions to a large extent, the flux of excess electrons may eventually overrun the Mehler-Asada cycle and ROS will accumulate. In the long term, free ROS will cause damage to the photosynthetic apparatus, affect numerous cellular functions, and eventually initiate leaf senescence (Desikan et al., 2001). Thus, one may expect that plants have developed mechanisms to match the capacity of the ETC to the metabolic electron demand.

At the molecular level, there exist indications for a concerted adjustment of light and carbon reactions. A decrease in the sink strength leads to accumulation of soluble sugars in the mesophyll, where they are perceived by a signaling network (sugar sensing; see Smeekens, 2000) and induce the depression of photosynthesis and the assimilatory metabolism (Pego et al., 2000; Paul and Foyer, 2001). Among others, genes coding for Rubisco and Rubisco activase, light-harvesting pro-

¹ This work was supported by the Studienstiftung des Deutschen Volkes (to M.A.S.) and by the Deutsche Forschungsgemeinschaft (to H.K.).

* Corresponding author; e-mail schoett@uni-muenster.de; fax 0049-251-8323823.

Article, publication date, and citation information can be found at www.plantphysiol.org/cgi/doi/10.1104/pp.104.052324.

teins, and plastocyanin (PC), are repressed in the high-sugar state (Pego et al., 2000; Oswald et al., 2001). Reduction of plastoquinone (PQ) and of the stromal thioredoxin system, a consequence of restricted Calvin cycle activity, represses photosynthetic genes (Pfannschmidt, 2003). Also, ROS formation itself was shown to repress genes encoding components of the light reactions, such as PSII, PSI, cytochrome (cyt)-*bf*, PC, and light-harvesting complexes (Foyer and Noctor, 2003; Gray et al., 2003).

While these studies were mainly at the level of gene expression, there is surprisingly little information about adaptive changes in the thylakoids at the level of the ETC. From studies with tobacco (*Nicotiana tabacum*) expressing Rubisco-antisense constructs, it was concluded that in plants with a reduced Calvin cycle activity, the electron flux through the Mehler-Asada pathway or into other alternative electron sinks was not enhanced. Instead, the PET capacity was adjusted to the assimilation rate (Ruuska et al., 2000). In barley (*Hordeum vulgare*; Burkey, 1994) and soybean (*Glycine max*; Burkey et al., 1996) genotypes with constitutively depressed assimilation, PET correlated with the PC content. While a number of information is available about the acclimation of thylakoids to light intensity (Anderson et al., 1988; Bailey et al., 2001) and quality (Chow et al., 1990; Kim et al., 1993), a consistent concept of a sink-control of PET does not yet exist.

Here, we analyze PET and the redox components of the ETC in thylakoids from tobacco var SNN leaves with a depressed carbon assimilation capacity. In one experiment, we studied the ETC from leaves of different ages. With increasing leaf age, the level of free carbohydrates increases, while the capacities of Calvin cycle and PET decrease (Ono et al., 2001; Yoshida, 2003). PSII (Prakash et al., 1998), cyt-*bf* (Ben-David et al., 1983; Holloway et al., 1983), and PSI (Humbeck et al., 1996; Miersch et al., 2000) have been discussed to be involved in the decline, but the actual flux control steps of PET have not yet been identified. In a second experiment, we studied the ETC in mature leaves from two transgenic plants with impaired sugar export from the mesophyll. In the A-41-10 transformant (Schaeuwen et al., 1990), photoassimilate export from source leaves is disturbed due to the overexpression of a yeast (*Saccharomyces cerevisiae*) invertase in the apoplast. Suc is hydrolyzed and the resulting hexoses are reimported into the mesophyll cells (Stitt et al., 1990). Furthermore, pathogenesis-related protein expression and hypersensitive responses are induced (Herbers et al., 1996) and ROS formation increases (Polle, 1996). In the PPA-4-80 transformant (Lerchl et al., 1995), phloem loading is impaired due to the ectopic expression of a pyrophosphatase from *Escherichia coli* in the companion cells. Here again, sugar accumulation in the mesophyll results in an early depression of Calvin cycle enzymes (Geigenberger et al., 1996).

We found that in leaves from both aging and sugar accumulating transgenic plants, the number of photosystems remained constant while the assimilation

capacity decreased. Instead, the content of cyt-*bf* and PC decreased with photosynthetic fluxes. We demonstrate that in thylakoids isolated from leaves with depressed (sink limited) carbon assimilation, the mobile electron carrier PC is an important factor controlling the PET flux.

RESULTS

Assimilation Rate during Leaf Aging

Assimilation and chlorophyll (chl) content were determined from leaves between the 5th and 24th leaf-generation of a wild-type plant, counted from top to bottom of the plant (Fig. 1). The plant had just started to flourish. Measurements were performed under both light- and CO₂-saturated conditions (10% CO₂). We have chosen these conditions as we can calculate the total assimilatory flux from oxygen evolution. Under physiological conditions, carbon assimilation may be limited by CO₂ and the total photosynthetic flux is partitioned between carbon assimilation and photorespiration.

The leaves of the 5th generation were not yet fully expanded (about 15 cm long) but exhibited a maximum chl content (per leaf area) and a high assimilation rate (relative to chl). The decline in the chl content (per leaf area) from the 5th to the 12th leaf generation was due to further leaf expansion. A further decline in chl (13th–24th generation) may be related to a stepwise reduction in the number of chloroplasts as leaf aging begins. The assimilation rate had its maximum around the 10th to 12th generation (280 mmol e⁻ mol chl⁻¹ s⁻¹) and then continuously declined with leaf age to 20% of its initial rate (22th–24th generation). Despite their depressed assimilation, these leaves had not yet entered the final phase of senescence, as they were still green and did not show chlorotic patches.

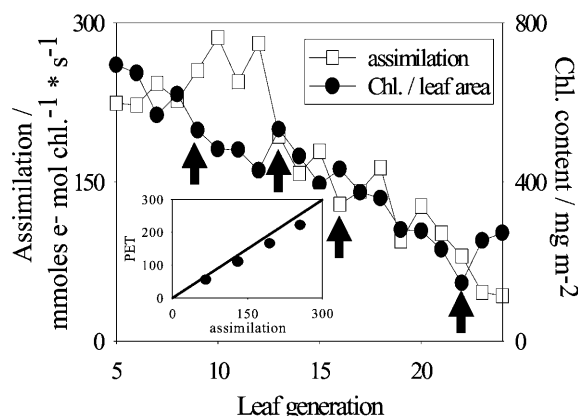


Figure 1. Assimilation rates in saturating light and chl content in dependence of leaf age. Leaf generations are counted from the top to the bottom of the plant. From leaves indicated by arrows, thylakoids were isolated and PET was measured. Inset, PET rates from thylakoids versus leaf assimilation.

Photosynthetic Electron Transport in Thylakoids Matches Leaf Assimilation

The electron transport capacity in thylakoids was measured in the presence of an uncoupler and with methylviologen (MV) as an electron acceptor. We selected these assay conditions, as we wanted to determine the PET capacity and exclude any mechanisms for short-term regulation of PET, such as photosynthetic control or high energy quenching. Chloroplasts were isolated from leaves of different ages as indicated by arrows in Figure 1. Under the conditions we used for the assimilation measurements (saturating CO_2), the vast majority of electrons provided by the ETC may be consumed by the carbon assimilation. Thus, in a first approximation, we could calculate the electron flux during leaf assimilation and compare it to the uncoupled PET rate in thylakoids (Fig. 1, inset). The relative changes in the thylakoid PET rate exactly followed those of electron flux rates during assimilation in leaves. The absolute PET rates in thylakoids were actually slightly (15%) below the flux rates in leaves. This is perhaps due to a small fraction of damaged thylakoids in the preparations, or to the fact that the standard measuring conditions for isolated thylakoids (pH, ionic milieu) may not necessarily be optimal for the electron flux rate. The F_v/F_m ratios determined from dark-adapted leaves were comparable with those in thylakoids isolated from these leaves (measured with a PAM-101 system; data not shown), suggesting that PSII was not damaged by the isolation procedure. The results indicate that the depression in the leaf assimilation is accompanied by a decline in the PET capacity at the thylakoid level.

Reaction Centers, Redox Components of the ETC, and Electron Flux Rates

Chl *a* and *b*, PSII (from C_{550}), and PSI (from P_{700}), as well as the other redox components of the ETC, were determined in thylakoids isolated from leaves of different ages. The chl *a/b* ratio and the numbers of the redox components, relative to chl, were plotted against the uncoupled PET. In wild-type plants, the PET rate in thylakoids decreased from about 280 (expanded young wild-type leaves) to 40 $\text{mmol e}^- \text{mol chl}^{-1} \text{s}^{-1}$ in aging leaves (compare with data in Fig. 1). From PPA-4-80 and A-41-10 transformants, we collected relatively young leaves (5th–10th generation) from plants exhibiting different levels of the phenotype. Transformants were reduced in growth rate, plant and leaf size, and expanded leaves developed characteristic patchy chlorosis and lesions. We collected leaves just before they had developed these symptoms. The different phenotype levels indicate different levels of sugar accumulation and Calvin cycle depression (Stitt et al., 1990). PET varied between about 150 $\text{mmol e}^- \text{mol chl}^{-1} \text{s}^{-1}$ in transformants with a moderate phenotype and less than 50 $\text{mmol e}^- \text{mol chl}^{-1} \text{s}^{-1}$ in plants with more severe phenotypes. We

did not use transformants exhibiting extreme phenotypes.

Over the whole range of fluxes, the content of PQ, and of redox-active PSII and PSI centers, relative to chl, remained stable (Fig. 2). The average number of PSII centers was 2.1 mmol mol chl^{-1} and that of PSI centers 2.4 mmol mol chl^{-1} (PSII to PSI = 0.88). The chl *a* to *b* ratio exhibited some variation between leaves around an average value of 3.4, but there was no significant change in dependence of the PET, suggesting that the overall ratio between light-harvesting complexes and core antennae of PSI and PSII remained relatively constant. The average content of PQ was about 8 to 9 mmol mol chl^{-1} . Despite some scatter, the data suggest a relatively stable PQ pool (Fig. 2).

However, *cyt-bf* and PC contents did vary over a wide range with flux rates (Figs. 3 and 4). The *cyt-bf* versus flux curves exhibits a slightly different shape for aging wild type or transformants. In the wild type (SNN), about 0.9 $\text{mmol cyt-bf mol chl}^{-1}$ correlated with the highest flux rates and remained relatively constant over the flux range of 280 to 180 $\text{mmol e}^- \text{mol chl}^{-1} \text{s}^{-1}$. At lower rates, *cyt-bf* decreased nearly linearly with fluxes to values as low as 0.2 $\text{mmol cyt-bf mol chl}^{-1}$ (Fig. 3). In transformants, the correlation was less pronounced compared to the wild type. In selected preparations, we compared the total of *cyt-bf* (from difference absorbance spectroscopy at selected redox potentials) with redox-active *cyt-bf* (from the amplitude of light-induced *cyt-f* redox transients in the presence of MV; data not shown). We found that the population of redox-active *cyt-bf* involved in PET was slightly (about 10%–15%) below the total content, suggesting that a small amount of the complexes may not actively contribute to the linear flux.

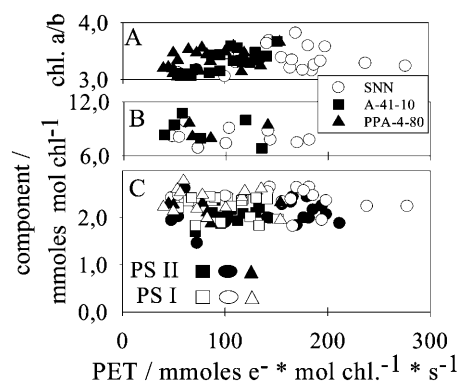


Figure 2. Chl *a/b* ratio (A), contents of PQ (B), and of PSII centers and PSI centers (P_{700}) relative to chl (C) versus the capacity of PET. All data obtained from isolated thylakoids. Circles, Wild type; squares, A-41-10 transformant; triangles, PPA-4-80 transformant. For wild type, thylakoids were isolated from leaves of different age. Highest PET rates were measured in thylakoids from leaves of the 5th to 12th generation. The PET rate decreases with leaf age (13th–24th generation). For transformants, thylakoids were isolated from young mature leaves only (5th–10th generation). Leaves were collected from different transformant plants. The transformants were heterozygous plants, which differed in the level of phenotypes and, hence, assimilation rates.

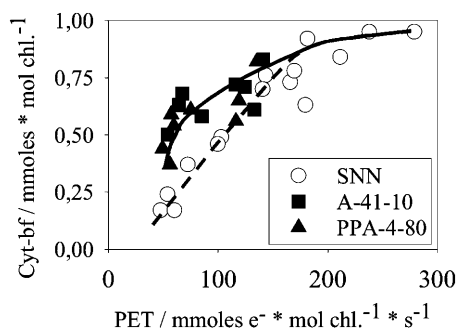


Figure 3. The *cyt-bf* content versus the rate of the light-saturated PET. All data were obtained from isolated thylakoids. Conditions and symbols as in Figure 2.

However, there was no indication that the relative proportions of redox-active and -inactive *cyt-bf* varied over the range of fluxes.

The mobile carrier PC exhibited a nearly linear relationship with the flux rate (Fig. 4). PC varied from about 12 mmol PC mol chl⁻¹ at high fluxes to less than 2 mmol PC mol chl⁻¹. This corresponds to PC:PSI ratios of almost 5 at high and 0.5 at very low flux rates. At high flux rates, PC still increased with the rate, while *cyt-bf* seemed to approach a maximum and, hence, the PC/*cyt-bf* ratio increased at high flux rates (compare Figs. 3 and 4). The maximum PC to P₇₀₀ ratios in young wild-type leaves are in agreement with numbers previously published for spinach (Haehnel et al., 1989) and barley (Burkey, 1994). The minimum values for PC contents shown here for sink-limited leaves are comparable to those published for low-light acclimated barley leaves (Burkey, 1993) and in soybean genotypes with constitutively repressed PET (Burkey et al., 1996).

High Potential Chain and Whole Chain Flux Rates

Figure 5 exhibits the relationship between the maximal whole chain flux rate from H₂O to the acceptor MV and the electron transport from *cyt-bf*, with duroquinol as an artificial donor, to MV. We isolated thylakoids from wild type and transformants as for the experiments shown in Figures 1 to 4. The two fluxes

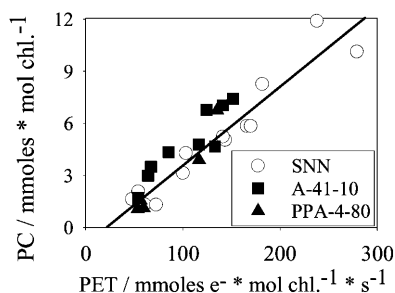


Figure 4. The PC content versus the rate of the light-saturated PET. Conditions and symbols as in Figure 2. The line represents a linear regression.

correlated in a linear way, suggesting that the whole chain flux (from water to MV) is controlled by the electron transport step from *cyt-bf* via PC to PSI (high potential chain).

Redox Kinetics of *Cyt-f*, PC, and P₇₀₀

In Figure 6, time-resolved redox kinetics of the individual reaction steps of the high potential chain in thylakoids are presented. Thylakoids were isolated from either fully expanded young or aged wild-type leaves. PET rates were 165 (young wild type) and 60 mmol e⁻ mol chl⁻¹ s⁻¹ (aged wild type). The content of P₇₀₀ remained constant, while PC declined from 8 in young to 1.6 mmol mol chl⁻¹ in old wild-type leaves (80% reduction). Redox-active *cyt-f* decreased from 1 to 0.45 mmol mol chl⁻¹ (about 57% reduction). Redox kinetics were measured in the presence of MV as PSI electron acceptor and with nigericine and nonactin as uncouplers.

After complete oxidation of the high potential chain by a saturating 100-ms light pulse, the dark relaxation kinetics of *cyt-f*, PC, and P₇₀₀ were followed. The noncorrected P₇₀₀ redox kinetics exhibited a slowly relaxing component (half-time [*t*_{1/2}] > 250 ms, about 15% of total P₇₀₀). As no such slow signals were observed in leaves (data not shown), we relate this slow phase to a small fraction of damaged thylakoids (see also discussion in Kirchhoff et al., 2004). Therefore, we subtracted the slow phases from the reduction kinetics, so that only *cyt-f*, PC, and P₇₀₀ involved in fast PET were considered for the further analysis. In the figure, all signals were normalized by setting the oxidized state at the end of the light pulse to one, and the reduced state (established after 500 ms) to zero. Recordings were displayed from the end of the light pulse (time zero).

The half-time of the slightly sigmoid P₇₀₀⁺ reduction kinetics increased from about 6 in thylakoids from young to 16 ms in thylakoids from old wild-type leaves, which reflects the observed decline in PET capacity (see above). In high-flux thylakoids, PC and *cyt-f* relaxed with halftimes of 20 and about 30 ms, respectively. In low-flux thylakoids, *cyt-f* relaxation exhibited a slight lag phase but, overall, was relatively little affected (*t*_{1/2} about 45 ms). A drastic change, however, was seen in the PC kinetics. Relaxation (*t*_{1/2} about 65 ms) was now slower than that of *cyt-f*. PC became even slightly oxidized in the dark before its reduction started with a 25-ms lag phase, in which almost all P₇₀₀⁺ had already been reduced. Obviously, about 10% of PC had not been oxidized during the pulse.

These results suggest that in thylakoids from aged wild-type leaves, the reoxidation of *cyt-f* is slowed down and the equilibration of PC and *cyt-f* is disturbed, compared to the situation in high flux thylakoids. This becomes more obvious in the equilibration plots displayed in Figure 7. Normalized values for oxidized PC from redox kinetics are plotted against

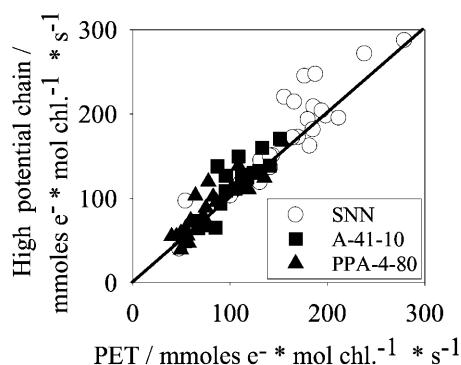


Figure 5. The light-saturated rate of the high potential chain, determined in the presence of DCMU, the electron donor duroquinol, and the acceptor MV. The rate was corrected for an electron leakage around the *cyt-bf* complex by determination of the rate in the presence of the *cyt-bf* inhibitor DMBIB (1 μ M). Symbols as in Figure 2.

those of *cyt-f*. From the resulting curves, apparent equilibrium constants (K_{app}) for the redox couple PC/*cyt-f* could be deviated (for details, see Kirchhoff et al., 2004). For high flux thylakoids, the value for K_{app} was 2.5, which agrees well with the reasonable assumption that the redox potential of PC is slightly more positive than that of *cyt-f*. In low-flux thylakoids, the apparent equilibrium constant was shifted to a 10-fold lower value ($K_{app} = 0.25$), suggesting that during dark relaxation the redox couple PC/*cyt-f* was out of its equilibrium.

PSII Activity and Whole Chain Electron Transport

In Figure 8, the light saturated PSII capacity was plotted against the whole chain flux. As expected, the reduction rate of the PSII acceptor by far exceeded that of the whole chain electron flux. Wild-type values scattered between 600 and 350 $\text{mmol e}^- \text{mol chl}^{-1} \text{s}^{-1}$, but did not show any significant correlation between PSII activity and whole chain flux. In transformants, however, the PSII activity showed a tendency to decline with the whole chain flux. In plants exhibiting a relatively strong phenotype, the PSII activity could be as low as 150 $\text{mmol e}^- \text{mol chl}^{-1} \text{s}^{-1}$. On the other hand, Figure 2 shows that the number of PSII centers, derived from the amplitude of the C_{550} signal, remained fairly constant. Obviously, in transformants, a large fraction of PSII could exist in an inactive state. The PSII activity assay with 2,5-dimethyl-1,4-benzoquinone (DMBQ) as an acceptor requires intact water splitting and primary electron-accepting PQ of PSII (Q_A)-acceptor sites. The C_{550} signal, however, reflects the very primary charge separation (Q_A reduction) occurring within the reaction center and does not require a functioning donor- and acceptor-site. Hence, the discrepancy between stable PSII contents, derived from the C_{550} signals, and the partially diminished DMBQ photoreduction may point to an impaired PSII donor- or acceptor-site in the transformants, possibly by photoinhibitory processes. This conclusion is further supported by the observation that the F_v/F_m ratios

of both dark-adapted leaves and isolated thylakoids decreased from about 0.8 in wild type with high photosynthesis to about 0.6 in transformants with reduced PET capacity (data not shown).

Assimilation Capacity and PC Content in Leaves

In Figure 9, the PC to PSI (P_{700}) ratio was plotted against leaf photosynthesis from O_2 evolution with saturating CO_2 as an acceptor. The PC and P_{700} transients were recorded in leaf discs and corrected for the related absorption coefficients. Over the whole range of fluxes, the PC/ P_{700} versus flux correlation was linear, in agreement with the result shown for thylakoids in Figure 4. The P_{700} content remained constant in all leaves (from P_{700} signals normalized to chl contents). When the PC to P_{700} ratio, determined in leaves, was multiplied with the average P_{700} content determined after thylakoid solubilization (Fig. 2), absolute PC contents of about 1 to 10 mmol mol chl^{-1} resulted, which is comparable to the absolute contents determined in thylakoids. Therefore, our method for PC quantification is also valid in planta.

DISCUSSION

Photosynthetic Electron Transport Adjusts to the Assimilation Capacity

In aging leaves, sugar export gradually decreases and soluble sugars increase (Ono et al., 2001; Yoshida, 2003). In the A-41-10 transformant, sugar is retained in leaves by an overexpressed yeast invertase in the apoplast, and in the PPA-4-80 transformant, phloem loading and sugar export is impaired to different levels. Thus, all kinds of leaves used in this study exhibited, at different levels, a high carbohydrate status and related depression of the Calvin cycle and carbon assimilation. Using these leaves or thylakoids isolated from these leaves, we could compare the number of thylakoid redox components, PET, and carbon fluxes from high-flux wild-type leaves and from leaves with depressed assimilation, and systematically correlate redox components of the ETC and fluxes.

PET flux rates were analyzed in the uncoupled state, which is a nonphysiological situation. With regard to the *in vivo* situation, the uncoupled rate may reflect, in a first approximation, the potential capacity of PET under conditions where ATP and NADPH are rapidly consumed by metabolic processes. We are aware that in the plant, the actual PET rate could be significantly below its capacity and may be adjusted by a number of regulatory feed-back processes, such as photosynthetic control during the induction phase of photosynthesis (for review, see Kramer et al., 1999). These kinds of short-term adjustments, however, are not in the focus of this study. Here, we study the potential capacity of the photosynthetic machinery of thylakoids as established after long term adjustment.

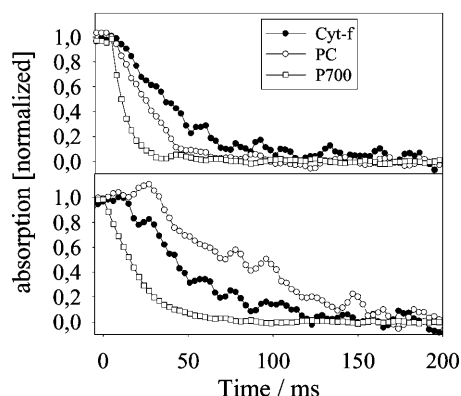


Figure 6. Light-induced redox kinetics of *cyt-f*, PC, and P_{700} in isolated thylakoids. A total of $100 \mu\text{M}$ MV, 10 mM ascorbate, $1 \mu\text{M}$ nigericine, and $0.5 \mu\text{M}$ nonactin were present. The reduction kinetics after the end of the actinic light pulse ($t = 0$) are shown. The original P_{700} recording revealed a slow phase ($t_{1/2} > 250 \text{ ms}$, about 15% of total signal), which was not observed in P_{700} recordings from leaves (data not shown). This slow phase was identified by fitting with an exponential function and mathematically omitted from the redox kinetics. The corrected redox kinetics were normalized (0 = reduced after 500 ms, 1 = oxidized state at the end of the light pulse). Thylakoids were isolated from young (A) and aged (B) wild-type leaves with high (A, $165 \text{ mmol e}^- \text{ mol chl}^{-1} \text{ s}^{-1}$) and low (B, $60 \text{ mmol e}^- \text{ mol chl}^{-1} \text{ s}^{-1}$) PET rates.

Over the whole range of assimilation capacity, the number of PSI and PSII (relative to chl *a* and *b*) remained constant (Figs. 2 and 9). This demonstrates that in low assimilation leaves a large potential overcapacity of photoreactions could exist. On the other hand, the depression in the carbon flux capacity is accompanied by a depression in the ETC such that the whole chain electron flux from water to PSI closely matches the assimilation capacity (Fig. 1, inset). Obviously, there is no substantial overflow of electrons through alternative pathways such as the Mehler-Asada cycle or the oxaloacetate/malate shuttle. Certainly, these pathways do play an important role in detoxification and fine adjustment of the chloroplast redox poise, but at least in the leaves used in this study, these reactions may not act as overflow valves to drain

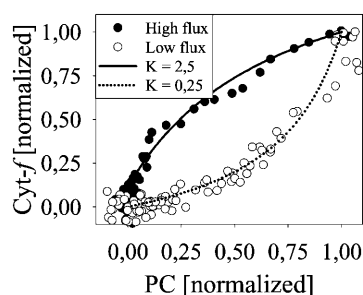


Figure 7. Redox equilibration plot of PC and *cyt-f* from wild-type thylakoids with high ($165 \text{ mmol e}^- \text{ mol chl}^{-1} \text{ s}^{-1}$) and low ($60 \text{ mmol e}^- \text{ mol chl}^{-1} \text{ s}^{-1}$) PET capacity (data from Fig. 6). Normalized redox signals of PC (x axis) were plotted against normalized redox signals of *cyt-f* (y axis). Apparent equilibrium constants (K_{app}) were calculated from the plots according to Kirchhoff et al. (2004).

large fluxes of excess electrons, when the assimilation capacity is reduced compared to the initial high assimilation state in expanded young leaves.

PC Exerts Control to the Electron Flux

Evidently, the high potential chain from *cyt-bf* to PSI, via the mobile redox-protein PC, exerts control to the whole chain flux (see Fig. 5). This raises the question about the factors controlling the flux. While PSI remains stable, both *cyt-bf* and PC decrease with flux, suggesting that these two components could be involved in the flux control. Decrease in *cyt-bf* with PET capacity is not a surprising result. There are numerous studies suggesting that PQ-reoxidation by the *cyt-bf* is the slowest step in PET and, hence, *cyt-bf* should be an important factor controlling the PET during various physiological conditions (e.g. Holloway et al., 1983; Anderson, 1992; Price et al., 1995). The *cyt-bf* versus flux correlation seems to be less stringent compared to PC, in particular in transformants (Figs. 3 and 4). At high fluxes, the number of *cyt-bf* seems to approach a maximum, while PC linearly increased with flux. The numbers for *cyt-bf* displayed in Figure 3 were obtained from difference absorbance spectra after complete equilibration at different redox potentials, and represent all *cyt-bf* included in the membrane, no matter whether they are involved in PET or not. The actual number of redox-active complexes included in the PET could be somewhat lower. We compared the total content of *cyt-bf* with that of redox-active *cyt-bf* [from light-induced *cyt-f* transients in the presence of MV and 3-(3,4-dichlorophenyl)-1,1-dimethylurea (DCMU); data not shown] and found that the contribution of redox-inactive *cyt-bf* may never exceed about 15% and, hence, may not significantly affect the *cyt-bf* versus flux correlations shown in this study. Obviously, under the particular conditions shown in this study, the electron flux is not as strictly related to the number of *cyt-bf* as one might expect.

On the other hand, the strictly linear correlation of PC over a wide range of fluxes shown in this study (Figs. 4 and 9) is striking. As we obtain the numbers for PC from light-induced redox kinetics in the presence of MV, all PC included in the analysis should participate in the linear flux. The ratio of PC:PSI decreases from 4 to 5 in leaves with high assimilation rates to values below 1 in leaves, whose assimilation is depressed. Although a general correlation between PC content and PET has already been reported for barley (Burkey, 1994) and soybean genotypes with constitutively depressed photosynthesis (Burkey et al., 1996), its role in flux control under physiological condition has not yet been established.

The strict PC versus flux correlation shown in this study per se is not a sufficient criterion for a PC flux control. If the PC reaction would be very fast, relative to whole chain flux, the correlation could be a coincidence and meaningless with regard to flux control.

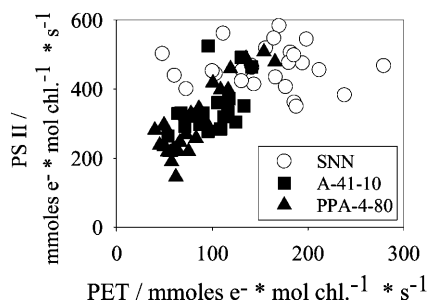


Figure 8. The capacity of PSII activity (measured as oxygen evolution in the presence of 2 mM DMBQ and 1 μ M nigericin) versus the capacity of PET. Symbols as in Figure 2.

The PC versus flux correlation would represent PC flux control only under the condition that the PC redox cycle is slow, relative to PET. Only in this case, the electron flux rate would be sensitive to the number of PC located in the thylakoid lumen. Electron transfers within the PC-PSI and PC-cyt-*bf* complexes are 10 to 100 times faster than quinone oxidation and, thus, cannot limit the flux (Drepper et al., 1996; Hope, 2000). However, there is indication that the lateral long-range diffusion of PC could be slow, compared to the light saturated whole chain flux (Haehnel, 1982, 1984). As the inner width of the thylakoid lumen (approximately 4 nm; Arvidsson and Sundby, 1999) and the size of the PC protein (approximately $4 \times 3 \times 3$ nm; Sigfridsson, 1998) are in the same order, a nonsufficient width of the diffusion space could restrict the lateral diffusion. An artificial reduction of the lumen width by hyperosmotic stress has been shown to nearly abolish PET, due to a severely impaired PC diffusion (Cruz et al., 2001).

A second limiting factor could be protruding proteins in the luminal diffusion space (Haehnel, 1984; Whitmarsh, 1986). In a preceding study, we already demonstrated that during fast PET, most of P_{700} (PSI centers) is actually out of the thermodynamic equilibrium with cyt-*f* and PC, suggesting restriction of PC migration (Kirchhoff et al., 2004). In a similar analysis (Figs. 6 and 7) we demonstrate a disequilibrium in the high-potential chain of low-flux thylakoids. In high flux thylakoids, PC and cyt-*f* relax almost in parallel. From the relaxation kinetics of cyt-*f* and PC, an apparent equilibrium constant, K_{app} of 2.5 was calculated. In thylakoids from aging leaves, PC reduction is delayed, compared to cyt-*f*, and starts after a time lag of about 30 ms, when most P_{700} is already reduced. During this lag-phase, PC (which was not completely oxidized during the pulse) even tends to become further oxidized, while cyt-*f* reduction proceeds. These two redox carriers seem to be out of their thermodynamic equilibrium as indicated by the 10-fold downward shift in the K_{app} (see Fig. 7). Obviously, reduction of cyt-*f* by plastoquinol (which is largely reduced in the light) occurs faster than its reoxidation by PC. Hence, reoxidation of cyt-*f* by PC, rather than the plastoquinol-oxidase activity of cyt-*bf*, limits the flux.

This could be due to a slow PC migration. Furthermore, any decline in cyt-*f*, relative to PSI, increases the number of PC redox cycles between cyt-*bf* and PSI required for the electron transport and, thus, would further aggravate a PC dependent flux restriction. Due to the low PC: P_{700} ratio in low flux thylakoids (more than $2 P_{700}/PC$), PC oxidation by P_{700} is thermodynamically even favored, compared to the situation in high-flux thylakoids. The efficient PC- P_{700} interaction explains why in these membranes PC could be kept oxidized in the dark until most of P_{700} was reduced. This further demonstrates that the flux must be restricted primarily by inefficient interaction between PC and cyt-*f*.

Flux control by PC adjustment (in concert with cyt-*bf*) results in a donor-site control of the PSI activity. This could be a safe way to control PSI, in particular in the low-assimilation leaves where its potential photochemical capacity very much exceeds the electron demand. Donor-site control would minimize over-reduction at the reducing site of PSI, which inevitably would lead to ROS production and, thus, would be potentially destructive. A mismatch due to a net shortage of electron donation to PSI reaction centers could be less damaging. P_{700} could accumulate in its oxidized form, P_{700}^+ . This species is a rather moderate oxidant and could act as a safe quencher of excess excitation energy (Ort, 2001). Safest for a leaf would be a close match of the PET and carbon flux capacity. On the other hand, PC flux control is expected to result in the accumulation of reduced PQ, which, in turn, is considered as a photoinhibitory condition for PSII, as will be discussed below.

Stability of PSI

PC is a small protein encoded in the nucleus where its gene is regulated by a number of physiological and metabolic signals. Regulation of *petE* (PC) gene expression in response to the chloroplast redox state (Sullivan and Gray, 2002; Pfannschmidt, 2003), soluble sugar (Oswald et al., 2001), ROS (Bolle et al., 1994), and

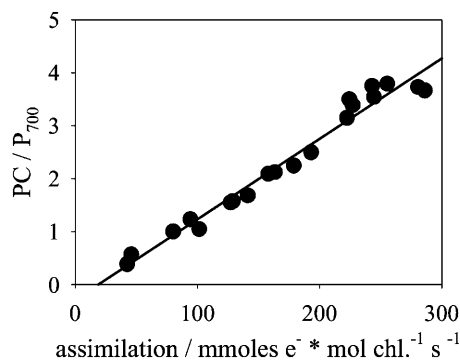


Figure 9. The leaf assimilation rate versus the PC/PSI (P_{700}) ratio. Data from wild-type plants shown in Figure 1. PC/P_{700} measurements were carried out with leaf discs, as described in Kirchhoff et al. (2004). The line represents a linear regression.

light is well documented. Compared to this, biosynthesis of PSI is extremely expensive. The complex consists of 18 subunits, encoded in the nuclear and chloroplast genome, contains a large number of cofactors, and more than 50 proteins may participate in its biosynthesis (Jensen et al., 2003). De novo synthesis of PSI is extremely slow. Photodamage by ROS, if it occurs, leads to degradation of PSI as a whole (Sonoike, 1996), and recovery takes more than a week and thus can diminish plant productivity severely (Tjus et al., 1998; Teicher et al., 2000; Kuduh and Sonoike, 2002). The stability of PSI during the large depression of the assimilation rate is striking (Figs. 2 and 9). In terms of energy costs, coordination of biosynthesis and regarding the timescale of adaptive responses, it seems to be more advantageous for the plant to control the activity rather than the number of PSI by adjusting the small PC protein.

Is PSII Activity Adjusted by Photoinhibition?

However, down-regulation of PC dependent fluxes will cause a potentially destructive overcapacity of the PSII photoreaction. Under such conditions, PQ and PSII acceptors are expected to become overreduced in high light and photoinhibition of PSII is likely to occur (Hideg et al., 2000). This may actually explain the gradual decline in the PSII activity and the F_v/F_m ratio observed in transformants but not in older wild-type leaves. As the overall number of PSII reaction centers remains fairly high in low assimilation leaves, there must be an increasing number of centers, which still exhibit a primary charge separation reaction (as indicated by the C_{550} signal; Fig. 2) but are no more able to transfer electrons from water to a quinone acceptor ($H_2O \rightarrow DMBQ$; Fig. 8). No such inhibition was seen in aged wild-type leaves where the number of centers, PSII activity, and the F_v/F_m ratio (not shown) remained high. Aged leaves are located in the lower parts of the plant, where photosynthetically active radiation could be as low as $50 \mu E m^{-2} s^{-1}$. These plants may be protected against photoinhibition by shading from younger leaves. We have not yet elucidated the mechanism of PSII inactivation, seen in the young mature leaves from transformants, and we do not know whether the inactivation is reversible or not. This decline in PSII activity might be regarded as a self-regulatory mild photoinhibition, by which PSII activity is adjusted to the reduced flux capacity. Different from PSI, PSII can easily be inactivated in high light by a number of reversible and irreversible mechanisms of photoinhibition or photodestruction. Inactivated PSII complexes are then reactivated or repaired rather than newly synthesized (Melis, 1999).

CONCLUSIONS

In this study, we demonstrate a coordinated decline in assimilation and PET capacity of leaves with re-

duced carbohydrate export (sink limitation) in such a way that the PET rate is well matched to the assimilation rate. Both *cyt-bf* and PC are adjusted to the flux in such a way that redox equilibration in the high potential chain of PC with *cyt-bf* is slowed down. PC, in concert with *cyt-bf*, is a key component that adjusts to control the PET flux. As the lateral PC diffusion in the lumen of grana stacks is relatively slow, the PET flux rate is sensitive to the number of PC, relative to *cyt-bf* and PSI. PC flux control may serve to adjust PET and protect PSI in high light against overreduction (and ROS production), in particular under conditions where the demand by the carbon assimilation is strongly diminished, as during sink limitation and sugar depression of photosynthesis and leaf aging. PC is the smallest redox protein in the ETC and could easily be adjusted by protein turnover control.

MATERIALS AND METHODS

Plants

Wild-type tobacco (*Nicotiana tabacum*) L. var Samsun NN was grown in a growth chamber (14 h light, $400\text{--}600 \mu E m^{-2} s^{-1}$, $24^\circ C$ day/ $16^\circ C$ night temperature). Transgenic tobacco plants (A-41-10; Schaewen et al., 1990; PPA-4-80, Lerchl et al., 1995) were provided by U. Sonnewald (Institute of Plant Genetics and Crop Plant Research [IPK], Gatersleben, Germany). Growth conditions for transgenic tobacco plants were as for wild-type plants, except that photosynthetically active radiation was $350 \mu mol quanta m^{-2} s^{-1}$.

Assimilation Rate in Leaves

Photosynthetic oxygen evolution was determined in leaf discs using a Clark-type oxygen-electrode (LD2; Hansatech Instruments, Norfolk, England). Leaf temperature was maintained at $20^\circ C$. Actinic light was applied by a tungsten halogen lamp (Schott, Mainz, Germany). To saturate the Rubisco with CO_2 , the leaf chamber was flushed with air containing 10% CO_2 and 5% O_2 .

Isolation of Thylakoids

Prior to thylakoid isolation, plants were kept in the dark for 24 h to reduce the starch content. After cutting out the major veins, four to six leaves were homogenized with a Waring Blendor in an isotonic medium containing 330 mM sorbitol, 1 mM $MnCl_2$, 5 mM $MgCl_2$, 40 mM KCl, and 50 mM MES, pH = 6.1. The homogenate was filtered through gauze (22- μm pore size) and centrifuged at 2,000g. The pellet was suspended in hypotonic medium (osmotic shock) containing 5 mM $MgCl_2$, 40 mM KCl, and 30 mM HEPES, pH = 7.6. After 30 s, an equal volume of hypertonic medium (5 mM $MgCl_2$, 40 mM KCl, 700 mM sorbitol, 30 mM HEPES, pH = 7.6) was added. The suspension was centrifuged at 200g, the supernatant at 2,000g. Resuspended thylakoids were stored in a medium containing 5 mM $MgCl_2$, 1 mM $MnCl_2$, 40 mM KCl, 330 mM sorbitol, and 50 mM HEPES, pH = 7.8.

Photosynthetic Electron Transport in Thylakoids

PET of a suspension of thylakoids was measured in a Clark-type oxygen electrode (Hansatech) at $20^\circ C$ in a medium containing 5 mM $MgCl_2$, 40 mM KCl, 330 mM sorbitol, and 30 mM HEPES, pH = 7.6. The actinic light was about $5,000 \mu E m^{-2} s^{-1}$. For whole chain electron transport, 100 μM MV, 1 mM $NaNO_3$, and 1 μM nigericin were added. For PSII activity, 2 mM DMBQ and 1 μM nigericin were added. The high-potential-chain was measured in the presence of 100 μM DCMU, 1 mM $NaNO_3$, and 1 μM nigericin with 1 mM duroquinone as donor and 100 μM MV as acceptor. The duroquinone \rightarrow MV flux was corrected

for an electron leakage after inhibition of the *cyt-bf* complex with 1 μM 2,5-dibromo-6-isopropyl-3-methyl-1,4-benzoquinone.

PSII Centers and P_{700}

Both PSII (C_{550}) and PSI (P_{700}) were determined after solubilization of thylakoids with 0.2% (w/v) of β -dodecyl-D-maltoside, so that optical artifacts resulting from light scattering, thylakoid energetization, and *cyt-bf*-based redox absorbance changes were eliminated. The number of redox-active PSII centers was determined from light-induced (100-ms pulse, 5,000 $\mu\text{E m}^{-2} \text{s}^{-1}$) changes in thylakoids at 540 minus 550 nm in the presence of 100 μM DCMU and 10 mM ferricyanide (C_{550} ; for details see Kirchhoff et al., 2002). The C_{550} -signal amplitude did not require a functional PSII-donor site, as was demonstrated by comparing C_{550} with inactive donor site (treatment with hydroxylamine; data not shown).

P_{700} was determined in the presence of 100 μM MV and 10 mM sodium ascorbate from light-pulse induced changes at 810 minus 860 nm using a PAM 101 photometer and an ED-P700DW emitter/detector unit (Walz, Efeltrich, Germany). The emitter/detector unit was connected by a bi-branched light guide to a reflecting (mirrored) and temperature-controlled steel chamber, as in (Kirchhoff et al., 2004). As this system determines both PC and P_{700} redox changes, contribution of PC was excluded by measuring at a pH of 4.8. At this pH, PC is rendered redox inactive, whereas P_{700} absorption is not affected. Under these conditions, we determined an absorption coefficient $\Delta\epsilon = 9.6 \text{ mM}^{-1} \text{ cm}^{-1}$ for P_{700} .

Cyt-*bf* and Redox-Active *cyt-f*

The total content of *cyt-bf* in a thylakoid preparation was determined by difference absorption spectra induced by step-wise addition of 1 mM ferricyanide, 10 mM sodium ascorbate, and 20 mM sodium dithionite. Signals were measured using a Hitachi U-3010 spectrophotometer (1-nm slit width, 580–520 nm). For further details, see Kirchhoff et al. (2002).

Redox kinetics of *cyt-f* were determined from light-pulse (100 ms, 5,000 $\mu\text{E m}^{-2} \text{s}^{-1}$) induced absorption changes (547 nm, 554 nm, 568 nm) in the presence of 100 μM MV, 10 mM sodium ascorbate, 1 μM nigericine, and 0.5 μM nonactin. Signals were deconvoluted as described by Kirchhoff et al. (2004).

PC Quantification and PC- P_{700} Redox Kinetics

The number of redox-active PC relative to P_{700} was derived from a deconvolution of differential light-pulse-induced absorption changes at 810 nm and 810 to 860 nm. Measurements with isolated thylakoids were performed in the presence of 100 μM MV, 10 mM sodium ascorbate, 1 μM nigericine, and 0.5 μM nonactin. Ascorbate keeps the high potential chain reduced in the dark. MV is an efficient electron acceptor for PSI that keeps P_{700} in the light oxidized. It also should keep ferredoxin (which could contaminate the near infrared signals) redox inactive. Electrochromic signals were eliminated by nigericine plus nonactin. The mathematical deconvolution and analysis of the signals is described by Kirchhoff and his coworkers (2004).

For a quantitative determination of PC relative to P_{700} in intact mesophyll, leaf discs were sprayed with a solution containing 10 mM MV, 1 mM DCMU, and 200 μM 2,5-dibromo-6-isopropyl-3-methyl-1,4-benzoquinone and 0.1% (v/v) Triton X-100 and then stored in a dark, moistened chamber for 45 min until measurements.

PQ

The chl-*a*-fluorescence induction (\pm DCMU) assay (Kirchhoff et al., 2000) was used to determine the PQ pool size. This assay gives a semiquantitative estimate of the PSII electron acceptors, relative to Q_A . The absolute PQ pool size was calculated by multiplication with the absolute number of PSII (from C_{550} -measurements).

Fluorescence induction was measured in a suspension of thylakoids (10 $\mu\text{g chl mL}^{-1}$) with a laboratory built fluorometer in the absence or presence of 20 μM DCMU at 5°C. Excitation light was filtered through heat reflectance filters and glass filters (Schott BG18 and Corning 9782). Emission was detected with a photomultiplier protected by a Schott AL 685 filter. To minimize reoxidation of electron acceptors by oxygen, the suspension was bubbled prior to the measurements with nitrogen. The areas above the induction curves

without DCMU, relative to that in presence of DCMU reflect the number of photoreduced PSII acceptors. Assuming that most electron acceptors in the high potential chain remain reduced, it may be taken, in a first approximation, as an estimate for the PQ pool. Fluorescence induction curves were analyzed according to Trissl and Lavergne (1994).

ACKNOWLEDGMENTS

We are grateful to Prof. Dr. Uwe Sonnwald (IPK, Gatersleben, Germany) for providing the tobacco transformants and to Julia Maurer (Institut für Botanik, Münster, Germany) for help during the establishment of the PC quantification method. We thank the reviewers for their helpful comments and suggestions.

Received August 24, 2004; returned for revision October 7, 2004; accepted October 7, 2004.

LITERATURE CITED

- Anderson JM (1992) Cytochrome *b_f* complex: dynamic molecular organization, function and acclimation. *Photosynth Res* 34: 341–357
- Anderson JM, Chow WS, Goodchild DJ (1988) Thylakoid membrane organization in sun / shade acclimation. *Aust J Plant Physiol* 15: 11–26
- Arvidsson PO, Sundby C (1999) A model for the topology of the chloroplast thylakoid membrane. *Aust J Plant Physiol* 26: 687–694
- Asada K (1999) The water-water cycle in chloroplasts: scavenging of active oxygen and dissipation of excess photons. *Annu Rev Plant Physiol Plant Mol Biol* 50: 601–639
- Backhausen JE, Kitzmann C, Horton P, Scheibe R (2000) Electron acceptors in isolated intact spinach chloroplasts act hierarchically to prevent over-reduction and competition for electrons. *Photosynth Res* 64: 1–13
- Badger MA, von Caemmerer S, Ruuska S, Nakamo H (2000) Electron flow to oxygen in higher plants and algae: rates and control of direct photoreduction (Mehler reaction) and Rubisco oxygenase. *Philos Trans R Soc Lond B Biol Sci* 355: 1433–1446
- Bailey S, Walters RG, Jansson S, Horton P (2001) Acclimation of *Arabidopsis thaliana* to the light environment: the existence of separate low light and high light responses. *Planta* 213: 794–801
- Ben-David H, Nelson N, Gepstein S (1983) Differential changes in the amount of protein complexes in the chloroplast membrane during senescence of oat and bean leaves. *Plant Physiol* 73: 507–510
- Bolle C, Sopory S, Lubberstedt T, Klosgen RB, Herrman RG, Oelmüller R (1994) The role of plastids in the expression of nuclear genes for thylakoid proteins studied with chimeric [β]-glucuronidase gene fusions. *Plant Physiol* 105: 1355–1364
- Burkey KO (1993) Effect of growth irradiance on plastocyanin levels in barley. *Photosynth Res* 36: 103–110
- Burkey KO (1994) Genetic variation of electron transport in barley: identification of plastocyanin as potential limiting factor. *Plant Sci* 98: 177–187
- Burkey KO, Gizlice Z, Carter TE Jr (1996) Genetic variation in soybean photosynthetic electron transport capacity is related to plastocyanin concentration in the chloroplast. *Photosynth Res* 49: 141–149
- Chow WS, Melis A, Anderson JM (1990) Adjustment of photosystem stoichiometry in chloroplasts improve the quantum efficiency of photosynthesis. *Proc Natl Acad Sci USA* 87: 7502–7506
- Cruz JA, Salbilla BA, Kanazawa A, Kramer DM (2001) Inhibition of plastocyanin to P_{700}^+ electron transfer in *Chlamydomonas reinhardtii* by hyperosmotic stress. *Plant Physiol* 127: 1167–1179
- Desikan R, Mackerness SAH, Hancock JT, Neill SJ (2001) Regulation of the *Arabidopsis* transcriptome by oxidative stress. *Plant Physiol* 127: 159–172
- Drepper F, Hippler M, Nitschke W, Haehnel W (1996) Binding dynamics and electron transfer between plastocyanin and photosystem I. *Biochemistry* 35: 1282–1295
- Foyer CH, Noctor G (2000) Tansley Review No. 112. Oxygen processing in photosynthesis: regulation and signaling. *New Phytol* 146: 359–388
- Foyer CH, Noctor G (2003) Redox sensing and signaling associated with reactive oxygen species in chloroplasts, peroxisomes and mitochondria. *Physiol Plant* 119: 355–364

- Geigenberger P, Lerchl J, Stitt M, Sonnewald U** (1996) Phloem-specific expression of pyrophosphatase inhibits long-distance transport of carbohydrates and amino acids in tobacco plants. *Plant Cell Environ* **19**: 43–55
- Gray JC, Sullivan JA, Wand JH, Jerome CA, MacLean D** (2003) Coordination of plastid and nuclear gene expression. *Philos Trans R Soc Lond B Biol Sci* **358**: 135–145
- Haehnel W** (1982) On the functional organization of electron transport from plastoquinone to photosystem I. *Biochim Biophys Acta* **682**: 245–257
- Haehnel W** (1984) Photosynthetic electron transport in higher plants. *Annu Rev Plant Physiol* **35**: 659–693
- Haehnel W, Ratajczak R, Robenek H** (1989) Lateral distribution and diffusion of plastocyanin in chloroplast thylakoids. *J Cell Biol* **108**: 1397–1405
- Herbers K, Meuwly P, Frommer WB, Metraux JP, Sonnewald U** (1996) Systemic acquired resistance mediated by ectopic expression of invertase: possible hexose sensing in the secretory pathway. *Plant Cell* **8**: 793–803
- Hideg E, Kalai T, Hideg K, Vass I** (2000) Do oxidative stress conditions impairing photosynthesis in the light manifest in photoinhibition. *Philos Trans R Soc Lond B Biol Sci* **355**: 1511–1516
- Holloway PJ, Maclean DJ, Scott KJ** (1983) Rate-limiting steps of electron transport in chloroplasts during ontogeny and senescence of barley. *Plant Physiol* **72**: 795–801
- Hope AB** (2000) Electron transfer amongst cytochrome *f*, plastocyanin and photosystem I: kinetics and mechanisms. *Biochim Biophys Acta* **1456**: 5–26
- Humbeck K, Quast S, Krupinska K** (1996) Functional and molecular changes in the photosynthetic apparatus during senescence of flag leaves from field-grown barley plants. *Plant Cell Environ* **19**: 337–344
- Jensen PE, Haldrup A, Roosgard L, Scheller HV** (2003) Molecular dissection of photosystem I in higher plants: topology, structure and function. *Physiol Plant* **119**: 313–321
- Kim JH, Glick RE, Melis A** (1993) Dynamics of photosystem stoichiometry adjustment by light quality in chloroplasts. *Plant Physiol* **102**: 181–190
- Kirchhoff H, Horstmann S, Weis E** (2000) Control of the photosynthetic electron transport by PQ diffusion microdomains in thylakoids of higher plants. *Biochim Biophys Acta* **1459**: 148–168
- Kirchhoff H, Mukherjee U, Galla HJ** (2002) Molecular architecture of the thylakoid membrane: Lipid diffusion space for plastoquinone. *Biochemistry* **41**: 4872–4882
- Kirchhoff H, Schöttler MA, Maurer J, Weis E** (2004) Plastocyanin redox kinetics in spinach chloroplasts: evidence for dis-equilibrium in the high potential chain. *Biochim Biophys Acta* **1659**: 63–72
- Kramer DM, Sacksteder CA, Cruz JA** (1999) How acidic is the lumen? *Photosynth Res* **60**: 151–163
- Kuduh H, Sonoike K** (2002) Irreversible damage to photosystem I in the light: cause of the degradation of chlorophyll after returning to normal growth conditions. *Planta* **215**: 241–248
- Lerchl J, Geigenberger P, Stitt M, Sonnewald U** (1995) Impaired photo-assimilate partitioning caused by a phloem-specific removal of pyrophosphate can be complemented by a phloem-specific cytosolic yeast-derived invertase in transgenic plants. *Plant Cell* **7**: 259–270
- Melis A** (1999) Photosystem II damage and repair cycle in chloroplasts: what modulates the rate of photodamage *in vivo*? *Trends Plant Sci* **4**: 130–135
- Miersch I, Heise J, Zelmer I, Humbeck K** (2000) Differential degradation of the photosynthetic apparatus during leaf senescence in barley (*Hordeum vulgare* L.). *Plant Biol* **2**: 618–623
- Ono K, Nishi Y, Watanabe A, Terashima I** (2001) Possible mechanism of adaptive leaf senescence. *Plant Biol* **3**: 201–209
- Ort DR** (2001) When there is too much light. *Plant Physiol* **125**: 29–32
- Ort DR, Baker NR** (2002) A photoprotective role of O₂ as an alternative electron sink in photosynthesis. *Curr Opin Plant Biol* **5**: 193–198
- Oswald O, Martin T, Dominy PJ, Graham IA** (2001) Plastid redox state and sugars: interactive regulators of nuclear-encoded photosynthetic gene expression. *Proc Natl Acad Sci USA* **98**: 2047–2052
- Paul MJ, Foyer CH** (2001) Sink regulation of photosynthesis. *J Exp Bot* **52**: 1383–1400
- Pego JV, Kortstee AJ, Huijser C, Smeekens SCM** (2000) Photosynthesis, sugars and the regulation of gene expression. *J Exp Bot* **51**: 407–416
- Pfannschmidt T** (2003) Chloroplast redox signals: how photosynthesis controls its own genes. *Trends Plant Sci* **8**: 33–41
- Polle A** (1996) Developmental changes in antioxidative systems in tobacco leaves as affected by limited sucrose export in transgenic plants expressing yeast-invertase in the apoplastic space. *Planta* **198**: 253–262
- Prakash JSS, Baig MA, Mohanty P** (1998) Alternations in electron transport characteristics during senescence of *Cucumis cotyledonary* leaves. Analysis of effects of inhibitors. *Photosynthetica* **35**: 345–352
- Price GD, Yu JW, von Caemmerer S, Evans JR, Chow WS, Anderson JM, Hurry V, Badger MR** (1995) Studying the central roles of the chloroplast cytochrome *b6/f* and ATP synthase complexes in transgenic tobacco: transformation with antisense RNA directed against the Rieske FeS and ATP δ nuclear encoded polypeptides. *Aust J Plant Physiol* **22**: 285–297
- Ruuska SA, Badger MR, Andrews TJ, von Caemmerer S** (2000) Photosynthetic electron sinks in transgenic tobacco with reduced amounts of Rubisco: little evidence for significant Mehler reaction. *J Exp Bot* **51**: 357–368
- Schaewen A, Stitt M, Schmidt R, Sonnewald U, Willmitzer L** (1990) Expression of a yeast-derived invertase in the cell wall of tobacco and Arabidopsis plants leads to accumulation of carbohydrate and inhibition of photosynthesis and strongly influences growth and phenotype of transgenic plants. *EMBO J* **9**: 3033–3044
- Sigfridsson K** (1998) Plastocyanin, an electron transfer protein. *Photosynth Res* **57**: 1–28
- Smeekens S** (2000) Sugar-induced signal transduction in plants. *Annu Rev Plant Physiol Plant Mol Biol* **51**: 49–81
- Sonoike K** (1996) Degradation of *psaB* gene product, the reaction center subunit of photosystem I, is caused during photoinhibition of photosystem I: possible involvement of reactive oxygen species. *Plant Sci* **115**: 157–164
- Stitt M, von Schaewen A, Willmitzer L** (1990) “Sink” regulation of photosynthetic metabolism in transgenic tobacco plants expressing yeast invertase in their cell wall involves a decrease of the Calvin-cycle enzymes and an increase of glycolytic enzymes. *Planta* **183**: 40–50
- Sullivan JA, Gray JC** (2002) Multiple plastid signals regulate the expression of the pea plastocyanin gene in pea and transgenic tobacco plants. *Plant J* **32**: 763–772
- Teicher HB, Moller BL, Scheller HV** (2000) Photoinhibition of PS I in field-grown barley (*Hordeum vulgare* L.): induction, recovery and acclimation. *Photosynth Res* **64**: 53–61
- Tjus SE, Moller BL, Scheller HV** (1998) PS I is an early target of photoinhibition in barley illuminated at chilling temperatures. *Plant Physiol* **116**: 755–764
- Trissl HW, Lavergne J** (1994) Fluorescence induction from photosystem II: analytical equations for the yields of photochemistry and fluorescence derived from analysis of a model including exciton-radical pair equilibrium and restricted energy transfer between photosynthetic units. *Aust J Plant Physiol* **22**: 183–193
- Whitmarsh J** (1986) Mobile electron carriers in thylakoids. In A Pirsson, MH Zimmermann, eds, *Encyclopedia of Plant Physiology*, Vol 19. Springer Verlag, Berlin, pp 508–525
- Yoshida S** (2003) Molecular regulation of leaf senescence. *Curr Opin Plant Biol* **6**: 79–84